https://doi.org/10.1016/j.jag.2018.02.002

Land Surface Temperature Trends as Indicator of Land Use Changes in Wetlands

Javier Muro[a,*], Adrian Strauch[a], Sascha Heinemann[d,c], Stefanie Steinbach[c], Frank Thonfeld[a,c], Björn Waske[b], Bernd Diekkrüger[c]

[a]*Center for Remote Sensing of Land Surfaces (ZFL), University of Bonn, Bonn 53113, Germany*
[b]*Institute of Geographical Sciences; Free University of Berlin, Berlin 12249, Germany*
[c]*Department of Geography, University of Bonn, Bonn 53113, Germany*
[d]*Institute of Bio- and Geosciences, Plant Sciences (IBG-2), Forschungszentrum Jülich GmbH, Germany*

Abstract

The impacts of agricultural expansion on wetlands are diverse and complex. Land surface temperature (LST) has a great potential to act as a global indicator of the status of wetlands and changes in their hydrological and evapotranspiration regimes, which are often linked to land use and cover changes. We use the whole MODIS LST archive (2000-2017) to perform time series analysis in the Kilombero catchment, Tanzania; a large wetland that has experienced major land conversions to agriculture during the last two decades. We estimated pixel based trends using three models: a seasonal trend model, and aggregated time series using annual means and percentile 90. We characterized the trends found by using land cover change maps derived from Landsat imagery and a post-classification comparison. The relation between NDVI (normalized difference vegetation index) and LST trends was also studied (r=-0.56). The results given by the seasonal trend model and annual means were similar (r=0.81). Fewer significant trends were found using the percentile 90, and these had larger magnitudes. Positive LST trends (i.e. increasing) corresponded to deforestation and farmland expansion into the floodplain, while forestation processes resulted in negative LST trends. Moderate increases of LST in natural wetlands suggest that the impacts of human activities extend also into non-cultivated areas. We provide evidence of how time series analysis of LST data can be successfully used to monitor and study changes in wetland ecosystems at regional and local scales.

Keywords: `monitoring`, wise use, LST, time series, MODIS
2017 MSC: 00-01, 99-00

*Principal corresponding author
Email addresses: `jmuro@uni-bonn.de` (Javier Muro), `astrauch@uni-bonn.de` (Adrian Strauch), `s.heinemann@fz-juelich.de` (Sascha Heinemann), `s.steinbach@uni-bonn.de` (Stefanie Steinbach), `frank.thonfeld@uni-bonn.de` (Frank Thonfeld), `bjoern.waske@fu-berlin.de` (Björn Waske), `b.diekkrueger@uni-bonn.de` (Bernd Diekkrüger)

1. Introduction

Wetlands are multiple value ecosystems, providing a wide variety of services (Tiner et al., 2015). In some cases, wetlands are almost the only source of natural resources sustaining rural economies. Their plant communities have widely varying vegetation type, density and water demand and availability. Their water requirements and impacts on streamflows are complex and uncertain, and agriculture practices have a large impact on their functioning. Remote sensing imagery has been widely used for monitoring wetlands and provide spatially distributed and temporally frequent information on their environmental state (Jones et al., 2009; Amler et al., 2015; Guo et al., 2017).

Most monitoring approaches are based on bi-temporal land use land cover (LULC) change techniques, or on mapping the water surface dynamics with optical ((Díaz-Delgado et al., 2016)) or radar time series ((Betbeder et al., 2015)). Thermal Infra-red data has been less frequently used, but it can nonetheless be essential to understand the spatial distributions of evapotranspiration in ground water dependent ecosystems. Land surface temperature (LST) based evapotranspiration estimations using thermal data have proven useful in practical applications in water management and water rights conflict solving (McVicar & Jupp, 1998; Anderson et al., 2012). It has been suggested that it is also possible to use LST variations to detect changes in land management practices, even when they are not associated with any direct change in land cover types (Luyssaert et al., 2014), or to map wetlands under aquatic vegetation (Leblanc et al., 2011). An additional advantage is that LST reacts to drought conditions earlier than NDVI (normalized difference vegetation index) (McVicar & Jupp, 1998).

A challenge encountered when using LST data is its high temporal variability; it greatly depends on climatic and illumination conditions, and measuring the change in LST between two single points in time is ecologically uninformative (McVicar & Jupp, 1998). Analyses of dense LST time series can reveal landscape change trends affecting water balances and energy fluxes. This is especially relevant in highly dynamic and water dependent ecosystems such as wetlands. Despite having a coarse resolution (1 km), the daily MODIS LST products are ideal for time series analysis, providing daily LST data at global scale since 2000 (Neteler, 2010).

A second challenge to overcome when analyzing LST time series is separating the seasonal, gradual, and abrupt changes that are combined in time series data (Verbesselt et al., 2010; Ghazaryan et al., 2016), in addition to the noise generated by atmospheric effects. Time series analysis can be performed by extracting and aggregating the data into statistical parameters (Forkel et al., 2013), performing harmonic analysis (Verbesselt et al., 2010; Forkel et al., 2013), or applying change detection algorithms and unsupervised classification of the changes (Hecheltjen et al., 2014). Methods such as BFAST (Breaks For Additive Seasonal and Trend) (Verbesselt et al., 2010), BFAST-monitor (Verbesselt et al., 2012), or greenbrown (Forkel et al., 2013, 2015) have been developed to deal with such challenges. They analyze data decomposing it into three components: the seasonal variation, trend, and a remainder (Verbesselt et al., 2010). Break points caused by sudden changes in the land cover properties are flagged.

A third challenge is caused by the irregular time steps caused by gaps due to clouds and other effects that result in poor pixel quality and are flagged as such in the quality band.

The open source R package greenbrown has been designed to analyze trends, trend changes, and phenology events in gridded time series of vegetation indices interpolating missing values. These indices are indicative of vegetation cover and health status, and widely used in time series analysis to assess changes in vegetation (Yengoh et al., 2015; Ghazaryan et al., 2016; Forkel et al., 2013). However, due to the highly variable surface water dynamics of some wetlands, vegetation indices are less suited to study their long term trends. Decreases in NDVI can be a result of a loss of vegetation, or consequence of an increase in flooding. On the other hand, both decreases in vegetation cover and water content will produce increases in LST and vice versa. In spite of that, we find fewer examples of the use of LST to monitor long term changes. When LST is used for monitoring, it is often in combination with NDVI (Julien et al., 2011) or is mainly focused on climatology (Jiménez-Muñoz et al., 2016). The relationship between NDVI and LST has also been previously studied; when energy is the limiting factor NDVI and LST have a positive correlation, but when water is the limiting factor LST and NDVI are negatively correlated (Karnieli et al., 2010). To our knowledge, despite its well-recognized potentials, LST has not yet been thoroughly employed to analyze temporal trends in water based ecosystems.

The objective of this research is to investigate the potential of LST as indicator of land use changes using the Kilombero Valley as a study area. The Kilombero Valley is a large complex of wetlands that has experienced major land conversions to agriculture during the last two decades, and the consequences of such conversions are not well understood. The spatio-temporal variations of LST and NDVI in Kilombero were analyzed and assessed against these land conversions using the full MODIS archive (2000-2017) of LST and NDVI products and a set of Landsat-based LULC change maps. Three different time series models were compared (annual means, annual maxima and a seasonal trend model), and the existence of break points in the time series was explored.

2. Materials and Methods

2.1. Study area

The Kilombero valley is a pilot site of the European Horizon 2020 project SWOS (Satellite-based Wetlands Observation Service) and the largest seasonal wetland in East Africa. The basin covers an area of 4,023,025 ha and the floodplain of the main river covers about 796,700 ha (Mombo et al., 2011). The elevation ranges between 200 and 2500 m.a.s.l. and the regional climate is sub-humid tropical with average daily temperatures around 22-23°C, and annual precipitation of about 1200 - 1400 mm. The bimodal rainy pattern comprises a short rainy season (November-January) and a long rainy season (March-May) with a distinct dry season from July until October (Koutsouris et al., 2016). The Kilombero River discharge is very variable (92 - 3044 m^3/s) and regularly floods the floodplain during the long rainy season.

The landscape consists of periodically inundated grasslands, swampy areas, Miombo woodlands, evergreen forest fragments, teak plantations, and an increasing farmed surface (Figure 1) (Leemhuis et al., 2017). Most of the agriculture is for subsistence and consists of maize and rice among other products. In the floodplain, there are two industrialized farms that produce sugar cane (Figure 1). The grasslands of the floodplain are periodically inundated, and during the dry season they are burnt to boost grass growth after the onset of the rainy season. Kilombero is a Ramsar site and home to several endangered and endemic species such as the puku antelope *(Kobus vardonii)*, which inhabits these frequently flooded grasslands. The floodplain also acts as a vital natural corridor between the Udzungwa Mountains National Park to the north-west and the Selous Game reserve in the east, and two of these wildlife corridors have recently ceased to function (Figure 1) (Wilson et al., 2017). The floodplain is also an important source of clean water for the downstream area (Wilson et al., 2017). Despite its long history of human occupation, the rapid increase in human population over the last decades (Tanzanian National Bureau of Statistics, 2012) along with uncontrolled farming practices have led to intensive land use conversion, wildlife decline and habitat fragmentation. A recent game census confirmed a strong decrease of large mammal populations (TWRI, 2013) and anecdotal evidence suggests decline in productivity of fisheries (Wilson et al., 2017). Furthermore, the agricultural expansion is altering the hydrological regime of the rivers, decreasing evapotranspiration and baseflow and increasing runoff (Leemhuis et al., 2017). The western part of the basin has a higher altitude and its vegetation cover has been degraded through frequent anthropogenic caused fires. As compensatory action, a few sites are being subjected to reforestation for climate change mitigation (GRL, 2009). Human population and industrialized agriculture are expected to increase due to plans for large scale agricultural development within the frame of SAGCOT (Southern Agricultural Growth Corridor of Tanzania) (Leemhuis et al., 2017).

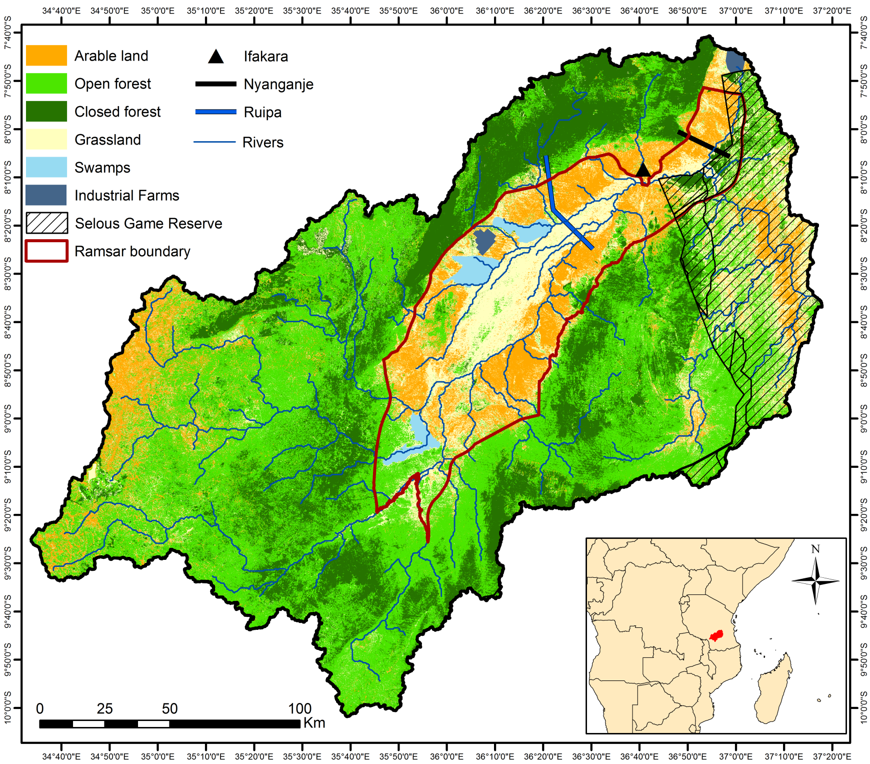

Figure 1: Kilombero catchment with its main LULC classes. Ifakara, is the main urban center. The map also shows the Nyanganje and Ruipa wildlife corridors, modified from (Wilson et al., 2017), and the Selous Game reserve

2.2. Datasets

We used the full archive (2000-2017) of the 8-day LST product (MOD11A2) from the Terra satellite. It is composed of the daily 1-kilometer LST product (MOD11A1) and stored on a 1-kilometer grid as the average values of clear-sky LSTs during an 8-day period. It uses the generalized split-window algorithm, optimized to separate ranges of atmospheric column water vapor and lower boundary air surface temperatures into tractable sub-ranges. Surface emissivities are estimated from land cover types and clouds are masked with the MODIS Cloud Mask data product (MOD35 L2). LST products are validated through field campaigns and radiance-based validation studies and are ready to use in science applications and publications. Errors are within ± 1 K in most cases, but larger errors may occur in desert regions due to the presence of aerosols. Further details regarding the validation are available at (Wan et al., 2004; Wan, 2008, 2014).

The NASA Land Processes Distributed Active Archive Center provides mainly 2 versions of the LST MOD11A2 product: V005 and V006. V006 seems to offer better estimates for arid areas (Wan, 2014), but V005 has been suggested to offer good quality data for inland water pixels (Neteler, 2010). Since our study area is a wetland, we used V005.

The NDVI dataset MOD13A1 from the Terra satellite is delivered every 16 days at 500 m resolution. It is retrieved from daily atmospherically corrected bidirectional surface reflectance products where low quality pixels are removed (Didan et al., 2017). The algorithm chooses the best available pixel value from all the acquisitions from the 16 day period.

We acquired Landsat Surface Reflectance Level-2 Science Products from the USGS downloading platform Earth Explorer and performed cloud masking using the Fmask algorithm (Zhu et al., 2015).

2.3. LULC change analysis

Multi-temporal statistical metrics (Mack et al., 2017) were calculated for the tasseled cap components of Wetness, Greenness, and Brightness (Crist & Cicone, 1984) from all available Landsat scenes of two three-year time spans; (2003-2005) and (2014-2016). A Land Use Land Cover (LULC) classification for each of these two time spans was performed using a Random Forest classifier, the Tasseled Cap components and the SRTM DEM and derivatives (slope, surface roughness, and Topographic Wetness Index (Beven & Kirkby, 1979)). Field observations and data from flight campaigns and Google Earth were used as reference for training and validation. Further information can be found in Leemhuis et al. (2017). The initial classification results were aggregated into coarser classes: Closed Forest, Open forest, Grasslands, Arable land and Water. A post classification comparison was performed between both LULC maps and error propagation was reduced by using a change-no change mask. This mask was produced applying a threshold (Otsu, 1979) on the magnitude component of a Change Vector Analysis of the tasseled cap 85 percentiles. Pixels labeled as “no change” in the mask were discarded from the post classification comparison. These pixels are assumed to be unchanged as changing labels of those pixels can be attributed to errors of the individual classifications. Further, LULC changes were clustered into three categories to facilitate the analysis and interpretation of results: Farmland Expansion on Grasslands (from Grasslands and Water to Arable Land), Deforestation (from Forest and Open Forest to Grasslands and Arable Land) and Forestation (from any class to Forest and Open Forest, and from Open Forest to Forest). We use the term “Forestation” to include “afforestation” (forest growth in previously non-forested areas) as well as “reforestation” (forest growth in previously vegetated areas). Changes in other directions were minimal and thus discarded. The overall accuracy of this LULC change map was estimated to be 60% (Table 1). It was evaluated using 200 points (of which only 158 were valid) randomly distributed and Google Earth, Bing, and Landsat imagery via Collect Earth (Bey et al., 2016).

Table 1: Accuracies of the LULC change map derived from Landsat scenes of two three-year time spans: 2003-2005 and 2014-2016

Accuracies	Deforestation	Forestation	Farmland Expansion	No Change	Total
Overall	-	-	-	-	60%
Users	60%	31%	58%	95%	61%
Producers	99%	100%	42%	13%	64%

2.4. Time Series analysis

The trend estimation of satellite data is usually performed in three ways (Forkel et al., 2013; Frey & Kuenzer, 2015); aggregating the data using multitemporal metrics, using an additive decomposition model, or via de-seasonalization of the data. Different methods might be used depending on the circumstances. We used three methods provided within the greenbrown R package (Forkel et al., 2013, 2015):

- Seasonal Trend Model (STM): Linear and harmonic terms are fitted to the original time series using ordinary least squares (OLS) regression. It is based on the classical additive decomposition model and follows the implementation of BFAST (Verbesselt et al., 2010). The significance of the trend is estimated using a t-test.
- Annual Aggregated Trends by annual means (AATmean). It calculates trends on annual aggregated time series using the annual mean and an OLS regression. The significance of the trend is estimated using the Mann-Kendall test.
- Annual Aggregated Trends using the percentile 90 (AAT90). It uses the annual 90 percentile and performs an OLS regression. The significance of the trend is also estimated using the Mann-Kendall test.

Trends were divided on a pixel basis into positive, negative or non-significant at 90% confidence level. Pixels with no significant trends were masked out (Figure 2). Our focus was to study the variation of LST with farmland expansion rather than the number of break points. Thus, we assumed monotonic trends and set the number of break points to 0. Additionally, to explore the influence of the number of breaks in the analysis we re-run the STM model setting the maximum number of break points to 1 (Figure 3). The break point detection algorithm searches for structural changes in a regression and estimates their position by minimizing the residual sum of squares (Forkel et al., 2013). When a break point is detected, the trend is divided into two segments whose slope may or may not be significant. To better estimate the position of a break point it is necessary to specify a minimum length of the segments. We set it to 2.5 years which represents 15% of the study period.

Records from complete years are needed when aggregating the data by annual means. Thus, data from 2000 and 2017 were excluded when comparing AATmean, AAT90 and STM models. However, further analyses were run using the STM and data from 2000 (from March 2000) and 2017 (to March 2017). To facilitate interpretation, the slopes of the trends were rescaled into ΔLST in Kelvin (K) using a linear regression;

$$\Delta LST = slope * t$$

where t is the length of the time period (or of each segment) in years.

We extracted LST data for homogeneous subsets of pixels representative of the spatial and temporal patterns of the area marked in Figure 3 a-g (industrial farmland expansion, swamp partially surrounded by agriculture, reforestation, subsistence farmland expansion, undisturbed wetland, seasonally inundated grassland and deforestation). To remove the influence of remaining unscreened clouds we eliminated the 5% of the lowest values, since clouds display lower LST. We plotted the LST data and calculated the times of break (Figure 4).

NDVI is widely used in time series analyses. However, LST is better suited to monitor changes in seasonally inundated areas since a drop in NDVI may be caused by an increase in surface water or by a decrease in vegetation. On the other hand, a drop in LST will be caused by a decrease of vegetation or water content (or both) and vice versa. To study the difference between NDVI and LST trends we compared the ΔLST map with a ΔNDVI map generated using the MODIS MOD13A1 product and the STM model.

3. Results

3.1. Models' performances

We compared the three models using only data from the period 2001-2016 to exclude years of incomplete data. AATmean and STM returned similar results regarding direction and magnitude of ΔLST (correlation coefficient r=0.81, Table 2). AAT90 reported fewer significant trends. These were generally in line with the other two models in terms of direction, but magnitude ranges had a greater amplitude (higher minimum and maximum values, Figure 2).

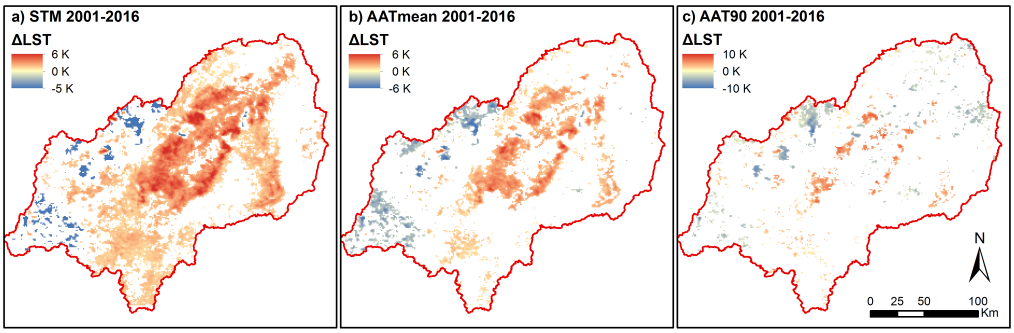

Figure 2: Results of the comparison of the three trend models used: a) Seasonal Trend Model (STM), b) Aggregated Time series by annual means (AATmean), and c) by percentile 90 (AAT90) at 90% confidence level. Monotonic trends were assumed for this analysis (i.e. break points were not searched for).

Table 2: Comparison of the results of the three trend models and their correlation to each other.

r	STM	AATmean	AAT90	SD
STM	1	0.81	0.52	1.17
AATmean	-	1	0.56	1.72
AAT90	-	-	1	4.1

3.2. *LST trends in Kilombero catchment*

We found average monotonic increases in LST of 2-3 K in the core of the Ramsar site (Figure 3A). Major increases of up to 6 K were found along the Ramsar boundary. The southern and northern parts of the Ramsar site showed lesser or no LST trends, as well as other areas further away from the Ramsar site. Mild decreases were found in a permanent swamp inside the Ramsar site ("b" in Figure 3 and Figure 4), and stronger decreases in some areas north-center and west of the basin that have been reforested with tree plantations during the study period ("c" in Figure 3 and Figure 4). When a break point was detected it was usually placed close to the start and end of the time series, except for a few areas to the east of the basin (red colors in Figure 3B).

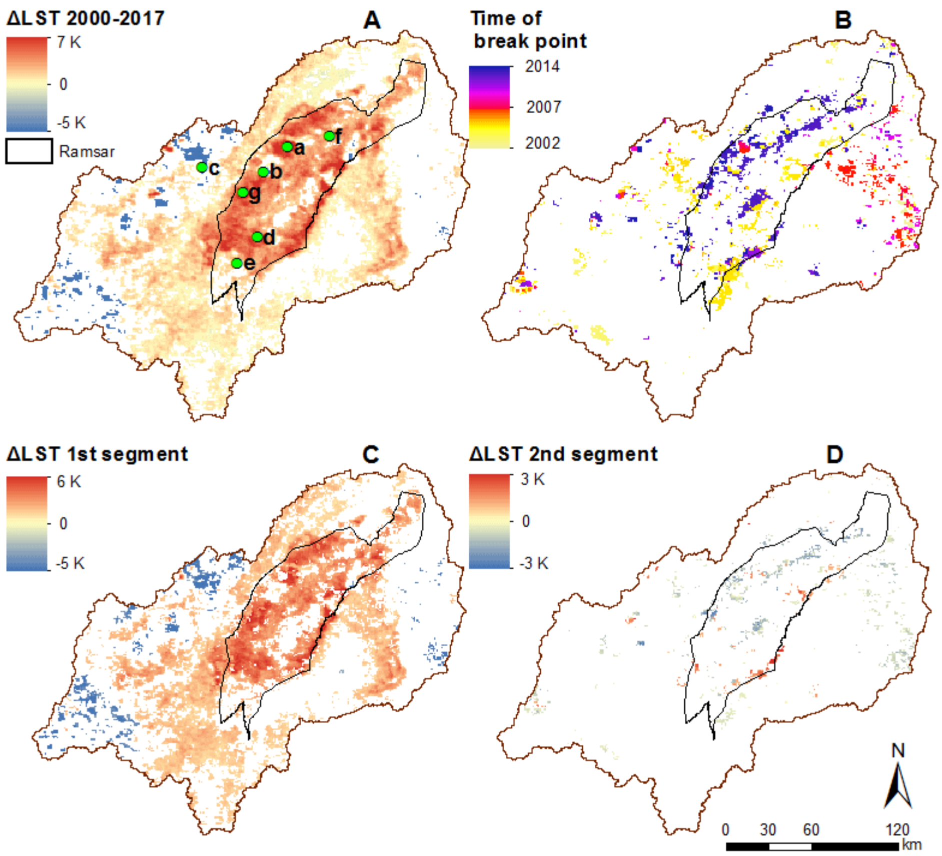

Figure 3: Results of the trend analysis using the STM model for the period March 2000 - March 2017. In map A, monotonic trends are assumed (i.e. break points = 0). In maps B, C and D the maximum number of break points was set to 1. B indicates the time of break, and C and D show the ΔLST before and after the break point respectively (i.e. first and second segment). Letters "a-g" mark the location of the pixels plotted in Figure 4.

We calculated and plotted the trend and break points for the points marked in Figure 3A as "a-g" and the results are shown in Figure 4. Point "a" corresponds to the expansion of a large scale farm of sugarcane on wetland area producing a break point. Point "b" is a permanent swamp that has not experienced land use changes during the study period, but it is surrounded by agriculture.

Here LST decreases after a break point in 2013 whose cause is unknown. Point “c” has been reforested with plantations, which has caused a break point and a very significant decreasing trend afterward ($p \leq 0.001$). Point “d” is an area where unorganized small scale farming has been developed during the study period. No break points are detected here, although the trend is increasing and very significant ($p \leq 0.001$). Point “e” is an undisturbed swamp that shows a very mild increasing trend significant only at 90% confidence interval. Point “f” is a seasonally inundated grassland that shows a similar temporal pattern than “e”. Point “g” is an upland forest that has been partly and slowly converted to small scale agriculture. A break point is detected in 2008 followed by a very significant increasing trend ($p \leq 0.001$).

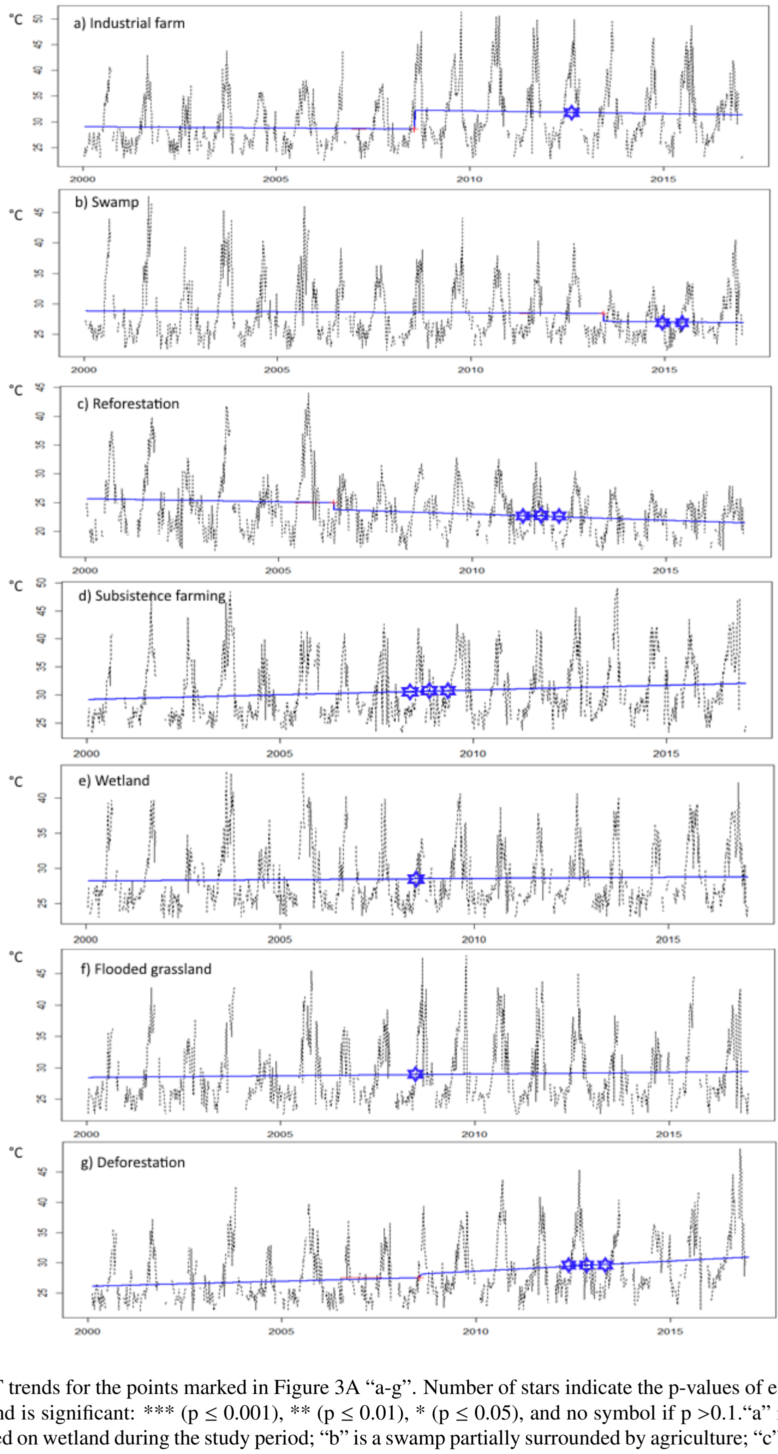

Figure 4: LST trends for the points marked in Figure 3A “a-g”. Number of stars indicate the p-values of each segment at which the trend is significant: *** ($p \leq 0.001$), ** ($p \leq 0.01$), * ($p \leq 0.05$), and no symbol if $p > 0.1$.“a” is an industrial farm developed on wetland during the study period; “b” is a swamp partially surrounded by agriculture; “c” is a reforested area; “d” is an area where small scale and unorganized farming has developed during the study period; “e” is a wetland up the river that is still mostly undisturbed; “f” is a seasonally inundated grassland; “g” was a forest upland area that has been converted to small scale agriculture.

3.3. LST, NDVI and LULC changes

The correlation analysis between ΔLST and ΔNDVI returned a correlation coefficient of -0.56. Only pixels with significant trends in both data sets were used ($p \leq 0.1$). Table 3 shows the statistics of both parameters. The mean and standard deviation of ΔLST and ΔNDVI per LULC change class are shown in the charts of Figure 5.

Table 3: Statistics of the ΔLST and ΔNDVI products

	Min	Max	Mean	SD
ΔLST	-5.3	6.9	1.68	1.12
ΔNDVI	-0.4061	0.4553	-0.0151	0.09

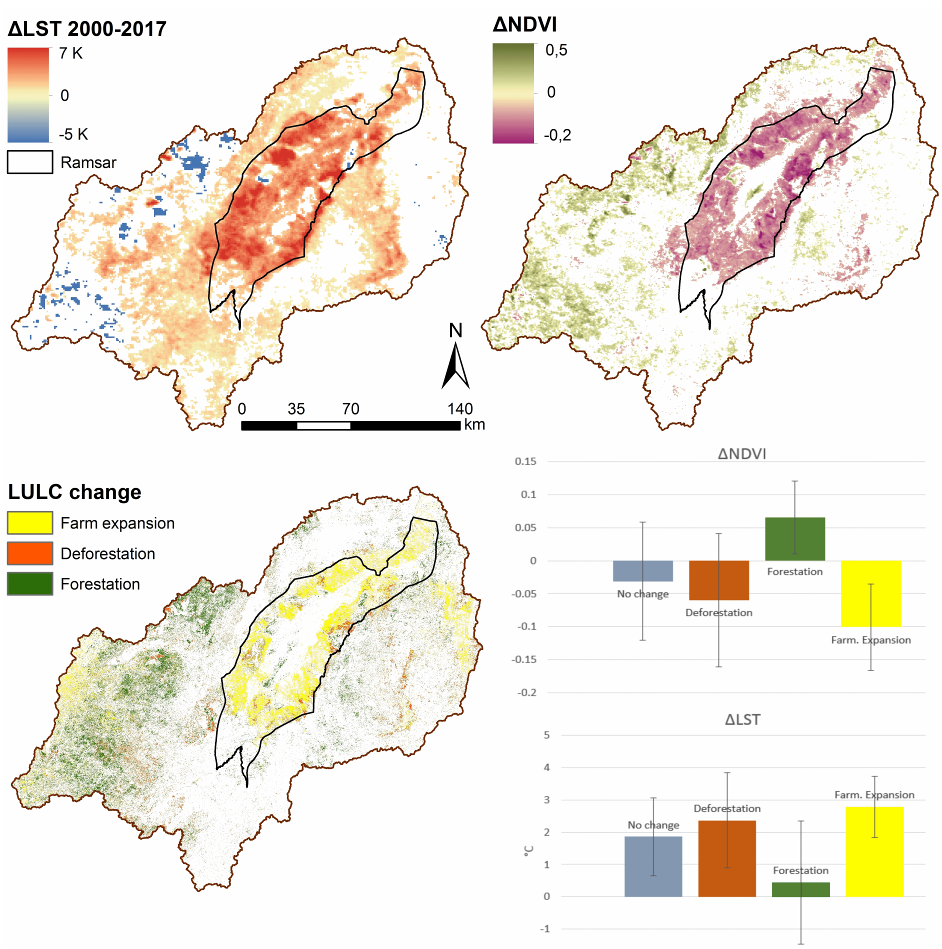

Figure 5: Variation of LST and NDVI in Kilombero using the STM model at 90% confidence interval for the period 2000-2017. Lower left map shows the LULC change map. ΔLST and ΔNDVI are grouped into the LULC change classes in the lower right charts.

The results of the trend analysis using the MODIS NDVI product revealed spatial patterns similar to those shown by the LST (Figure 5). The largest increases in LST and decreases in NDVI took place inside or close to the Ramsar site. There were, however, some differences between ΔLST and ΔNDVI. For instance, there were no significant trends of NDVI in the core of the Ramsar site, whereas the LST trend analysis indicated positive and significant monotonic trends ("f" in Figure 3 and 4).

Despite the differences in spatial resolution between datasets (1 km for ΔLST, 500 m for ΔNDVI and 30 m for the LULC maps) Deforestation and Farmland Expansion patterns were related to significant increases in LST (Figure 5 lower right chart). Overall, Farmland Expansion on grasslands was responsible for an increase of almost 3 K (±1), and Deforestation caused increases of more than 2 K (±1.5). Areas labeled as "No change" also experienced overall increases in LST. Pixels showing decreasing LST trends corresponded mostly to Forestation processes (Figure 2c and 3c). However, the overall patterns of Forestation found in the LULC change maps could not be associated with trends in LST (Figure 5). On the other hand, increases in NDVI were related to the change class Forestation, and decreases to Farmland Expansion.

4. Discussion

4.1. Models' performances

The three models (STM, AATmean and AAT90) agree in the vast concentric area at the outer limits of the Kilombero river floodplain (Figure 2). There is also a common area of LST decrease in the northern central part of the catchment product of forestation projects. AATmean and STM produced similar results in terms of magnitude and direction of ΔLST (Figure 2 and Table 2), but the number of pixels with significant trends was larger using the STM model. Aggregating time series data is a common way to account for the seasonality and it is resilient against overestimation of trends (Forkel et al., 2013). However, it reduces the number of observations which may result in an underestimation of the trend significance. It will also prevent us from studying intra-annual dynamics such as beginning, end or length of the season (Forkel et al., 2013; Frey & Kuenzer, 2015; Ghazaryan et al., 2016).

The AAT90 model reported fewer pixels with significant trends but with much larger amplitudes (Table 2). The AAT90 method, by its definition, has a focus on the trend of the annual peak LST which is when changes in vegetation cover or water content are expected to have a more pronounced effect in the LST. STM and AATmean (directly or indirectly) account for the same time an area is left bare without vegetation (e.g. after a harvest). Hence, STM and AAT mean are more sensitive the LULC changes than AAT90. This does not necessarily mean that AAT90 is less accurate. Wetlands are crucial during the dry periods in many parts of the world serving as refuge and source of water in moments of scarcity. Mapping ΔLST only during the LST peak season can still have relevant applications for specific cases, such as inferring the availability of water or vegetation during breeding periods of fish, amphibians, or vectors of diseases (Metz et al., 2014), or during migrations of birds and other animals. These three time series analysis methods involve advantages and constraints that will be more or less relevant depending on the application (Forkel et al., 2013). In general, we recommend the use of seasonal trend models rather than aggregation methods because the seasonal trend models allow using data for incomplete years and at full temporal resolution.

Break points represent abrupt changes either due to conversion of one land cover type to another or due to changes in land management (Forkel et al., 2013; Verbesselt et al., 2010), e.g., through implementation or abandonment of irrigation systems (Hentze et al., 2017). However, land use changes often have long-term impacts on biophysical variables such as productivity or LST rather than abrupt ones. Hence, long-term monitoring and a combination of break point detection and trend estimation is required to characterize LULC changes and their impact on LST. Whether break points are detected or not, partly depends on the parameters set. For instance, the minimum length of a segment determines the shortest length of time necessary for a break point to be detected. If it is a large value (e.g. 40% of the study period), break points towards the beginning or end of the time series will not be detected, or will be placed somewhere else in the time line. On the other hand, a small minimum length might return false break points at the beginning or end of the time series. The use of different trend models also had an effect on where a break point was set for some of the sampling sites “a-g” (Figure 4). This is expected since we are measuring the trends of different properties (e.g. extreme or average values). Since the focus of the paper is to evaluate the effect of land changes on LST and due to the relatively short length of the study period, a thorough study of the break points was not carried out.

4.2. LST trends in Kilombero catchment

Disturbances like deforestation cause a break point in the time series, increasing the LST abruptly. It would be expected that LST showed a decreasing trend during the years after deforestation as vegetation begins to regrow. However, in cases of substitution of natural vegetation (whether it is forest or wetland) for agriculture, LST tended to keep increasing after the break point (Figure 4g and d). In our case, Farmland Expansion was also related to increases in LST, contributing to create an agricultural heat island (Raymond et al., 1994). Most of the trends found were monotonic, and most of the break points identified were close to the end or beginning of the time series (Figure 3B).

The large increase in population in the area along with lack of property rights have caused uncontrolled farmland expansion as well as deforestation (Jones et al., 2009; Connors, 2015; Wilson et al., 2017). Most of the increases in LST and agricultural expansion patterns took place along the borders of the Ramsar area where many natural resources are found (mainly water, wood, and fertile lands). Areas of permanent swamps (Figure 3c and 4c) and at the south of the Ramsar site are still not heavily used and showed no major increases in LST (nor decreases in NDVI). The seasonally inundated grasslands of the core of the Ramsar site have remained unoccupied, mostly because recurrent floods limit agricultural expansion. However, they present moderate increases in LST, (although not in NDVI), which suggests that farming activities might be affecting the water balance in these seasonally inundated areas. This is in agreement with the results obteined in Leemhuis et al. (2017), where hydrological models determined that the land cover changes are decreasing evapotranspiration and baseflow and increasing runoff. This is also supported by the fact that the Selous Game Reserve (Figure 1) is the only larger region without a significant LST trend. As a game reserve it is not foreseen to host humans, limiting human impact compared to the regions outside protected areas. Climate change processes could also be affecting the evapotransporation regimes of the floodplain, but 17 years is too short time for such conclusions.

When transforming the continuous patterns of the land surface into discrete classes, errors are bound to occur. In our case, the Forestation class was overestimated (Table 2). Because of that and the large difference in spatial resolution between the LULC change map (30 m) and the LST data-set (1 km), overall changes in LST for the Forestation class were not conclusive. However, in areas where the ground truth data showed actual forestation of grasslands the LST decreased considerably (Figure 4c). For the other classes of land change the results were clearer: LST increased in areas of Deforestation and Farmland Expansion, and areas without LULC changes also reported significant increments in LST.

It is to be noted that the recently released annual LULC products from the Climate Change Initiative still consider a large part of the floodplain as flooded grasslands, despite that it is rather heavily used for agriculture and its ecological functions have been degraded (Leemhuis et al., 2017). The concepts of "Ecological Character" and "Wise Use" of wetlands defined by the Ramsar Convention imply that wetland ecosystem services may be exploited to a certain extent, as long as the integrity and health of the wetland system remain uncompromised (Verhoeven & Setter, 2010). Our results, along with those of other researches (Connors, 2015; Willcock et al., 2016; Wilson et al., 2017; Leemhuis et al., 2017) indicate that agricultural expansion might be compromising the wetland's ecological character. The uncontrolled use of the wetland for agriculture might even have repercussions on areas that are still mostly natural, such as the core of the floodplain (Figure 5).

The upcoming plans to modernize the agriculture in the area by SAGCOT should consider the water balance and the preservation of the ecosystem services that the wetland provides (Leemhuis et al., 2017). For instance, modernizing the energy sources that farmers use might stop or reduce the deforestation caused by the use of timber for fuel. One of the main ecological functions of the Kilombero floodplain was to serve as a corridor for wildlife between the Udzungwa Mountains National Park to the northwest, and the Selous Game reserve to the east (Figure 1). That function has been recently lost, leaving animal populations isolated (Wilson et al., 2017). Two of these now defunct corridors (Ruipa and Nyanganje, Figure 1) used to go through the areas where LST has increased. Restoring Ruipa and Nyanganje corridors would be a straight forward solution regarding the connectivity function. There are a few areas that show no increase in LST, suggesting that they are not yet heavily used by agriculture and could be subjected to some regime of protection. Evidence suggests that protection regimes in the area have succeeded in stopping deforestation and farmland expansion to some extent (Willcock et al., 2016; Brink et al., 2016). However, if migration continues, different approaches might be needed to provide sustainable strategies for the wise use of the wetland.

4.3. Potentials and limitations of LST time series

MODIS LST time series can be useful for local and regional scale applications despite its coarse spatial resolution. ΔLST maps would not be useful for wetlands smaller than 1 x 1 km, but single pixel trend analysis can still produce meaningful results. Besides, there is also room for improvements in spatial resolution. For instance, future efforts could be directed towards combining MODIS with Landsat (Weng et al., 2014) or ASTER data (Yang et al., 2016) for time series analysis at higher spatial resolution.

Despite the MODIS cloud mask, intermittent cloudiness and low quality pixels might still affect the surface temperature. In this study area, high mountain ridges are almost always cloudy, and trends there are questionable. Using only the high quality pixels of MODIS might be advisable in very arid areas where the cloud mask tends to fail, although it might reduce the number of observations considerably. Recent studies also show that other cloud mask schemes perform better (Gomis-Cebolla et al., 2016).

Trend analysis carry a risk of over- and underestimation, and quantitative results should be treated with care. STM models offer the possibility of using data from incomplete years, but are prone to overestimation. Aggregated time series are more resilient against overestimation, but the data used is reduced, generating a risk of underestimation.

5. Conclusions

The impacts of agricultural expansion and deforestation on wetlands are diverse and complex. Sometimes, certain impacts will not affect the classification of a land cover (e.g., wood extraction of single trees rather than stand replacing clear-cuts), but will have an impact on its biophysical variables (productivity, spectral indices or LST). The spatial and temporal distribution of such impacts in wetlands can be analyzed by using LST dense time series. These analyses can also be particularly useful in large areas with high rates of expansion and difficult access to field data, delivering quantitative information in a timely manner.

Analyses based on annual means (AATmean) and the seasonal trend model (STM) performed similarly in our case, with the STM identifying more pixels with significant trends. The analysis based on peak temperatures (AAT90) detected areas of extreme change. Overall increases in LST matched farmland expansion and deforestation patterns, and LST and NDVI were negatively correlated. We observed increases of LST also in unoccupied areas of the Ramsar site, where agriculture and the number of cattle herders have rapidly increased during the last decade, suggesting that their impact extends into the still natural areas.

The time period studied here is too short to consider the influence of climate change. However, we do provide evidence on how the agricultural expansion on wetlands increases the surface temperature, which in turn determines the atmospheric temperature.

Operational production of LST trend maps and time series charts can provide wetland managers with a quick and reliable single indicator of the effect of land processes on water and energy fluxes.

Acknowledgments

The SWOS project has received funding from the European Union's Horizon 2020 research and innovation program under Grant Agreement No. 642088. The contents of this paper are the sole responsibility of the authors and can in no way be taken to reflect the views of the European Union. Aerial images for classification and training were provided by Ian Games and Giuseppe Daconto, from the Kilombero and Lower Rufiji Wetlands Ecosystem Management Project (KILORWEMP). KILORWEMP is financed by the European Union and Belgian Aid and executed by the Ministry of Natural Resources and Tourism of Government of Tanzania and the Belgian Development Agency (TAN1102711). We also express our gratitude to the GlobE - Wetlands in East Africa project funded by the German Federal Ministry of Education and Research (FKZ: 031A250 A-H), with additional funding provided by the German Federal Ministry of Economic Cooperation and Development. We thank the 3 anonymous reviewers and editor whose comments helped improve the quality of the manuscript.

References

Amler, E., Schmidt, M., & Menz, G. (2015). Definitions and Mapping of East African Wetlands: A review. *Remote Sensing*, *7*, 5256–5282. URL: `http://www.mdpi.com/2072-4292/7/5/5256/`. doi:`10.3390/rs70505256`.

Anderson, M. C., Allen, R. G., Morse, A., & Kustas, W. P. (2012). Use of Landsat thermal imagery in monitoring evapotranspiration and managing water resources. *Remote Sensing of Environment*, *122*, 50–65. URL: `http://linkinghub.elsevier.com/retrieve/pii/S0034425712000326`. doi:`10.1016/j.rse.2011.08.025`.

Betbeder, J., Rapinel, S., Corgne, S., Pottier, E., & Hubert-Moy, L. (2015). TerraSAR-X dual-pol time-series for mapping of wetland vegetation. *ISPRS Journal of Photogrammetry and Remote Sensing*, *107*, 90–98. URL: `http://linkinghub.elsevier.com/retrieve/pii/S0924271615001380`. doi:`10.1016/j.isprsjprs.2015.05.001`.

Beven, K. J., & Kirkby, M. J. (1979). A physically based, variable contributing area model of basin hydrology. *Hydrological Sciences Bulletin*, *24*, 43–69. URL: http://www.tandfonline.com/doi/abs/10.1080/02626667909491834. doi:10.1080/02626667909491834.

Bey, A., Snchez-Paus Díaz, A., Maniatis, D., Marchi, G., Mollicone, D., Ricci, S., Bastin, J.-F., Moore, R., Federici, S., Rezende, M., Patriarca, C., Turia, R., Gamoga, G., Abe, H., Kaidong, E., & Miceli, G. (2016). Collect Earth: Land use and land cover assessment through augmented visual interpretation. *Remote Sensing*, *8*, 807. URL: http://www.mdpi.com/2072-4292/8/10/807. doi:10.3390/rs8100807.

Brink, A., Martínez-López, J., Szantoi, Z., Moreno-Atencia, P., Lupi, A., Bastin, L., & Dubois, G. (2016). Indicators for assessing habitat values and pressures for protected areas: An integrated habitat and land cover change approach for the Udzungwa Mountains National Park in Tanzania. *Remote Sensing*, *8*, 862. URL: http://www.mdpi.com/2072-4292/8/10/862. doi:10.3390/rs8100862.

Connors, J. P. (2015). Agricultural development, land change, and livelihoods in Tanzania's Kilombero Valley. URL: https://repository.asu.edu/attachments/164069/content/Connorsasu0010E15455.pdf.

Crist, E. P., & Cicone, R. C. (1984). A physically-based transformation of Thematic Mapper data—the TM Tasseled Cap. *IEEE Transactions on Geoscience and Remote Sensing*, *GE-22*, 256–263. URL: http://ieeexplore.ieee.org/document/4157507/. doi:10.1109/TGRS.1984.350619.

Díaz-Delgado, R., Aragons, D., Afn, I., & Bustamante, J. (2016). Long-term monitoring of the flooding regime and hydroperiod of Doñana marshes with Landsat time series (19742014). *Remote Sensing*, *8*, 775. URL: http://www.mdpi.com/2072-4292/8/9/775. doi:10.3390/rs8090775.

Didan, K., Barreto Munoz, A., Solano, R., & Huete, A. (2017). MODIS vegetation index users guide. URL: https://vip.arizona.edu/documents/MODIS/MODIS_VI_UsersGuide_June_2015_C6.pdf.

Forkel, M., Carvalhais, N., Verbesselt, J., Mahecha, M., Neigh, C., & Reichstein, M. (2013). Trend change detection in NDVI time series: Effects of inter-annual variability and methodology. *Remote Sensing*, *5*, 2113–2144. URL: http://www.mdpi.com/2072-4292/5/5/2113/. doi:10.3390/rs5052113.

Forkel, M., Migliavacca, M., Thonicke, K., Reichstein, M., Schaphoff, S., Weber, U., & Carvalhais, N. (2015). Codominant water control on global interannual variability and trends in land surface phenology and greenness. *Global Change Biology*, *21*, 3414–3435. URL: http://dx.doi.org/10.1111/gcb.12950. doi:10.1111/gcb.12950.

Frey, C. M., & Kuenzer, C. (2015). Analysing a 13 years MODIS Land Surface Temperature time series in the Mekong Basin. In C. Kuenzer, S. Dech, & W. Wagner (Eds.), *Remote Sensing Time Series* (pp. 119–140). Springer International Publishing volume 22. URL: http://link.springer.com/10.1007/978-3-319-15967-6{_}6.

Ghazaryan, G., Dubovyk, O., Kussul, N., & Menz, G. (2016). Towards an improved environmental understanding of land surface dynamics in Ukraine based on multi-source remote sensing time-series datasets from 1982 to 2013. *Remote Sensing*, *8*, 617. URL: http://www.mdpi.com/2072-4292/8/8/617. doi:10.3390/rs8080617.

Gomis-Cebolla, J., Jiménez-Muñoz, J., & Sobrino, J. A. (2016). MODIS-based monthly LST products over Amazonia under different cloud mask schemes. *Data*, *1*, 2. URL: http://www.mdpi.com/2306-5729/1/2/2. doi:10.3390/data1020002.

GRL (2009). Reforestation in grassland areas of Uchindile, Kilombero, Tanzania and Mapanda, Mufindi, Tanuania. URL: https://theredddesk.org/sites/default/files/ufp_mfp_ccba_02_10_09-1.pdf.

Guo, M., Li, J., Sheng, C., Xu, J., & Wu, L. (2017). A review of wetland remote sensing. *Sensors*, *17*, 777. URL: http://www.mdpi.com/1424-8220/17/4/777. doi:10.3390/s17040777.

Hecheltjen, A., Thonfeld, F., & Menz, G. (2014). Recent advances in remote sensing change detection a review. In I. Manakos, & M. Braun (Eds.), *Land Use and Land Cover Mapping in Europe* (pp. 145–178). Springer Netherlands volume 18. URL: http://link.springer.com/10.1007/978-94-007-7969-3_10 DOI: 10.1007/978-94-007-7969-3_10.

Hentze, K., Thonfeld, F., & Menz, G. (2017). Beyond trend analysis: How a modified breakpoint analysis enhances knowledge of agricultural production after zimbabwe's fast track land reform. *International Journal of Applied Earth Observation and Geoinformation*, *62*, 78–87. URL: http://linkinghub.elsevier.com/retrieve/pii/S0303243417301101. doi:10.1016/j.jag.2017.05.007.

Jiménez-Muñoz, J. C., Mattar, C., Sobrino, J. A., & Malhi, Y. (2016). Digital thermal monitoring of the Amazon forest: an intercomparison of satellite and reanalysis products. *International Journal of Digital Earth*, *9*, 477–498. URL: https://www.tandfonline.com/doi/full/10.1080/17538947.2015.1056559. doi:10.1080/17538947.2015.1056559.

Jones, K., Lanthier, Y., van der Voet, P., van Valkengoed, E., Taylor, D., & Fernndez-Prieto, D. (2009). Monitoring and assessment of wetlands using earth observation: The GlobWetland project. *Journal of Environmental Management*, *90*, 2154–2169. URL: http://linkinghub.elsevier.com/retrieve/pii/S0301479708000364. doi:10.1016/j.jenvman.2007.07.037.

Julien, Y., Sobrino, J. A., Mattar, C., Ruescas, A. B., Jiménez-Muñoz, J. C., Sória, G., Hidalgo, V., Atitar, M., Franch, B., & Cuenca, J. (2011). Temporal analysis of Normalized Difference Vegetation Index (NDVI) and Land Surface Temperature (LST) parameters to detect changes in the Iberian land cover between 1981 and 2001. *Interna-*

tional Journal of Remote Sensing, *32*, 2057–2068. URL: http://www.tandfonline.com/doi/abs/10.1080/01431161003762363. doi:10.1080/01431161003762363.

Karnieli, A., Agam, N., Pinker, R. T., Anderson, M., Imhoff, M. L., Gutman, G. G., Panov, N., & Goldberg, A. (2010). Use of NDVI and Land Surface Temperature for drought assessment: Merits and limitations. *Journal of Climate*, *23*, 618–633. URL: http://journals.ametsoc.org/doi/abs/10.1175/2009JCLI2900.1. doi:10.1175/2009JCLI2900.1.

Koutsouris, A. J., Chen, D., & Lyon, S. W. (2016). Comparing global precipitation data sets in Eastern Africa: a case study of Kilombero Valley, Tanzania: Comparing global precipitation data sets in Tanzania, East Africa. *International Journal of Climatology*, *36*, 2000–2014. URL: http://doi.wiley.com/10.1002/joc.4476. doi:10.1002/joc.4476.

Leblanc, M., Lemoalle, J., Bader, J.-C., Tweed, S., & Mofor, L. (2011). Thermal remote sensing of water under flooded vegetation: New observations of inundation patterns for the "Small" Lake Chad. *Journal of Hydrology*, *404*, 87–98. URL: http://linkinghub.elsevier.com/retrieve/pii/S0022169411002642. doi:10.1016/j.jhydrol.2011.04.023.

Leemhuis, C., Thonfeld, F., Näschen, K., Steinbach, S., Muro, J., Strauch, A., López, A., Daconto, G., Games, I., & Diekkrüger, B. (2017). Sustainability in the Food-Water-Ecosystem Nexus: The Role of Land Use and Land Cover Change for Water Resources and Ecosystems in the Kilombero Wetland, Tanzania. *Sustainability*, *9*, 1513. URL: http://www.mdpi.com/2071-1050/9/9/1513. doi:10.3390/su9091513.

Luyssaert, S., Jammet, M., Stoy, P. C., Estel, S., Pongratz, J., Ceschia, E., Churkina, G., Don, A., Erb, K., Ferlicoq, M., Gielen, B., Grnwald, T., Houghton, R. A., Klumpp, K., Knohl, A., Kolb, T., Kuemmerle, T., Laurila, T., Lohila, A., Loustau, D., McGrath, M. J., Meyfroidt, P., Moors, E. J., Naudts, K., Novick, K., Otto, J., Pilegaard, K., Pio, C. A., Rambal, S., Rebmann, C., Ryder, J., Suyker, A. E., Varlagin, A., Wattenbach, M., & Dolman, A. J. (2014). Land management and land-cover change have impacts of similar magnitude on surface temperature. *Nature Climate Change*, *4*, 389–393. URL: http://www.nature.com/doifinder/10.1038/nclimate2196. doi:10.1038/nclimate2196.

Mack, B., Leinenkugel, P., Kuenzer, C., & Dech, S. (2017). A semiautomated approach for the generation of a new land use and land cover product for Germany based on Landsat time-series and LUCAS *in-situ* data. *Remote Sensing Letters*, *8*, 244–253. URL: https://www.tandfonline.com/doi/full/10.1080/2150704X.2016.1249299. doi:10.1080/2150704X.2016.1249299.

McVicar, T. R., & Jupp, D. L. (1998). The current and potential operational uses of remote sensing to aid decisions on drought exceptional circumstances in Australia: a review. *Agricultural Systems*, *57*, 399–468. URL: http://linkinghub.elsevier.com/retrieve/pii/S0308521X98000262. doi:10.1016/S0308-521X(98)00026-2.

Metz, M., Rocchini, D., & Neteler, M. (2014). Surface temperatures at the continental scale: Tracking changes with remote sensing at unprecedented detail. *Remote Sensing*, *6*, 3822–3840. URL: http://www.mdpi.com/2072-4292/6/5/3822/. doi:10.3390/rs6053822.

Mombo, F., Speelman, S., Van Huylenbroeck, G., Hella, J., Pantaleo, M., & Moe, S. (2011). Ratification of the Ramsar convention and sustainable wetlands management: Situation analysis of the Kilombero Valley wetlands in Tanzania. *Journal of Agricultural Extension and Rural Developmen t*, *3(9)*, 153–164. URL: http://www.academicjournals.org/journal/JAERD/article-abstract/709ED8C1710.

Neteler, M. (2010). Estimating Daily Land Surface Temperatures in Mountainous Environments by Reconstructed MODIS LST Data. *Remote Sensing*, *2*, 333–351. URL: http://www.mdpi.com/2072-4292/2/1/333/. doi:10.3390/rs1020333.

Otsu, N. (1979). A threshold selection method from gray-level histograms. *IEEE Transactions on Systems, Man, and Cybernetics*, *9*, 62–66. URL: http://ieeexplore.ieee.org/document/4310076/. doi:10.1109/TSMC.1979.4310076.

Raymond, W. H., Rabin, R. M., & Wade, G. S. (1994). Evidence of an Agricultural Heat Island in the Lower Mississippi River Floodplain. *Bulletin of the American Meteorological Society*, *75*, 1019–1025. doi:10.1175/1520-0477(1994)075<1019:EOAAHI>2.0.CO;2.

Tanzanian National Bureau of Statistics (2012). National bureau of statistics tanzania census 2012. URL: http://dataforall.org/dashboard/tanzania/.

Tiner, R. W., Lang, M. W., & Klemas, V. V. (2015). In *Remote Sensing of Wetlands: Applications and Advances* chapter 1. (p. 4). CRC Press. URL: http://www.crcnetbase.com/doi/book/10.1201/b18210 DOI: 10.1201/b18210.

TWRI (2013). *Aereal census of large animals in the Selous-Mikumi Ecosystem*. Technical Report Tanzania Wildlife Research Institute. URL: http://www.daressalam.diplo.de/contentblob/4102454/Daten/3821641/DownloadReportSelousElephants.pdf.

Verbesselt, J., Hyndman, R., Newnham, G., & Culvenor, D. (2010). Detecting trend and seasonal changes in satellite image time series. *Remote Sensing of Environment*, *114*, 106–115. URL: http://linkinghub.elsevier.com/retrieve/pii/S003442570900265X. doi:10.1016/j.rse.2009.08.014.

Verbesselt, J., Zeileis, A., & Herold, M. (2012). Near real-time disturbance detection using satellite image time series. *Remote Sensing of Environment*, *123*, 98–108. URL: http://linkinghub.elsevier.com/retrieve/pii/S0034425712001150. doi:10.1016/j.rse.2012.02.022.

Verhoeven, J. T. A., & Setter, T. L. (2010). Agricultural use of wetlands: opportunities and limitations. *Annals of Botany*, *105*, 155–163. URL: https://academic.oup.com/aob/article-lookup/doi/10.1093/aob/mcp172. doi:10.1093/aob/mcp172.

Wan, Z. (2008). New refinements and validation of the MODIS Land Surface Temperature/Emissivity products. *Remote Sensing of Environment*, *112*, 59–74. URL: http://linkinghub.elsevier.com/retrieve/pii/S0034425707003665. doi:10.1016/j.rse.2006.06.026.

Wan, Z. (2014). New refinements and validation of the collection-6 MODIS land-surface temperature/emissivity product. *Remote Sensing of Environment*, *140*, 36–45. URL: http://linkinghub.elsevier.com/retrieve/pii/S003442571300285X. doi:10.1016/j.rse.2013.08.027.

Wan, Z., Zhang, Y., Zhang, Q., & Li, Z.-L. (2004). Quality assessment and validation of the MODIS global land surface temperature. *International Journal of Remote Sensing*, *25*, 261–274. URL: http://www.tandfonline.com/doi/abs/10.1080/0143116031000116417. doi:10.1080/0143116031000116417.

Weng, Q., Fu, P., & Gao, F. (2014). Generating daily land surface temperature at Landsat resolution by fusing Landsat and MODIS data. *Remote Sensing of Environment*, *145*, 55–67. URL: http://linkinghub.elsevier.com/retrieve/pii/S0034425714000479. doi:10.1016/j.rse.2014.02.003.

Willcock, S., Phillips, O. L., Platts, P. J., Swetnam, R. D., Balmford, A., Burgess, N. D., Ahrends, A., Bayliss, J., Doggart, N., Doody, K., Fanning, E., Green, J. M. H., Hall, J., Howell, K. L., Lovett, J. C., Marchant, R., Marshall, A. R., Mbilinyi, B., Munishi, P. K. T., Owen, N., Topp-Jorgensen, E. J., & Lewis, S. L. (2016). Land cover change and carbon emissions over 100 years in an African biodiversity hotspot. *Global Change Biology*, *22*, 2787–2800. URL: http://doi.wiley.com/10.1111/gcb.13218. doi:10.1111/gcb.13218.

Wilson, E., McInnes, R., Mbaga Damas, P., & Ouedraogo, P. (2017). Ramsar advisory mission report/; Kilombero Valley Ramsar Site. URL: http://www.ramsar.org/sites/default/files/documents/library/ram83_kilombero_valley_tanzania_2016_e.pdf.

Yang, G., Weng, Q., Pu, R., Gao, F., Sun, C., Li, H., & Zhao, C. (2016). Evaluation of ASTER-like daily Land Surface Temperature by fusing ASTER and MODIS data during the HiWATER-MUSOEXE. *Remote Sensing*, *8*, 75. URL: http://www.mdpi.com/2072-4292/8/1/75. doi:10.3390/rs8010075.

Yengoh, G. T., Dent, D., Olsson, L., Tengberg, A. E., & Tucker, C. J. (2015). Use of the normalized difference vegetation index (NDVI) to assess land degradation at multiple scales. In *Use of the Normalized Difference Vegetation Index (NDVI) to Assess Land Degradation at Multiple Scales* (pp. 1–7). Springer International Publishing. URL: http://link.springer.com/10.1007/978-3-319-24112-8{_}1 DOI: 10.1007/978-3-319-24112-8_1.

Zhu, Z., Wang, S., & Woodcock, C. E. (2015). Improvement and expansion of the fmask algorithm: cloud, cloud shadow, and snow detection for Landsats 47, 8, and Sentinel-2 images. *Remote Sensing of Environment*, *159*, 269–277. URL: http://linkinghub.elsevier.com/retrieve/pii/S0034425714005069. doi:10.1016/j.rse.2014.12.014.